



Contents lists available at ScienceDirect

Science Bulletin

journal homepage: www.elsevier.com/locate/scib

Article

Sub-basin scale inhomogeneity of mantle in the South China Sea revealed by magnesium isotopes

Yuan Zhong^a, Guo-Liang Zhang^{a,b,c,*}, Qi-Zhen Jin^d, Fang Huang^d, Xiao-Jun Wang^e, Lie-Wen Xie^f

^a Center of Deep Sea Research, Institute of Oceanology, Chinese Academy of Sciences, Qingdao 266071, China

^b Laboratory for Marine Geology, National Laboratory for Marine Science and Technology (Qingdao), Qingdao 266237, China

^c Center for Ocean Mega-Science, Chinese Academy of Sciences, Qingdao 266071, China

^d CAS Key Laboratory of Crust-Mantle Materials and Environments, School of Earth and Space Sciences, University of Science and Technology of China, Hefei 230026, China

^e State Key Laboratory of Continental Dynamics, Department of Geology, Northwest University, Xi'an 710069, China

^f State Key Laboratory of Lithospheric Evolution, Institute of Geology and Geophysics, Chinese Academy of Sciences, Beijing 100029, China

ARTICLE INFO

Article history:

Received 28 May 2020

Received in revised form 30 November 2020

Accepted 30 November 2020

Available online xxx

Keywords:

Mantle heterogeneity
Mid-ocean-ridge basalt
Magnesium isotope
Hainan plume
South China Sea

ABSTRACT

The South China Sea (SCS) is the largest extensional basin in the western Pacific and was formed after rifting of the Euro-Asian continental margin. The nature of its underlying mantle remains enigmatic due to the lack of sampling of the seafloor's igneous crust. The International Ocean Discovery Program Expedition 349 cored seafloor basalts of the southwestern (Site U1433) and eastern (Site U1431) SCS sub-basins. The recovered basalt samples exhibit different source lithologies and geochemistries. The Mg isotopic compositions of seafloor basalts from these sites were investigated to elucidate the origin of this large-scale mantle inhomogeneity. Results indicate that the Site U1431 basalts have a mantle-like average $\delta^{26}\text{Mg}$ value of $-0.27\text{‰} \pm 0.06\text{‰}$ (2SD; $n = 10$). Together with inhomogeneous Sr-Nd-Pb-Hf isotopic compositions, the Site U1433 basalts have an average $\delta^{26}\text{Mg}$ value ($-0.20\text{‰} \pm 0.06\text{‰}$; 2SD; $n = 8$) higher than those of the Site U1431 basalts and normal mantle. Their heavier Mg isotopic compositions and low $^{206}\text{Pb}/^{204}\text{Pb}$ ratios (~ 17.7) indicate that the Site U1433 basalts were affected by the re-melting of detached continental-arc lithosphere in the sub-ridge mantle. The coupling of Mg and Sr-Nd isotopes provides robust evidence that the mantle-like $\delta^{26}\text{Mg}$ values of the Site U1431 basalts resulted from mixing between detached continental arc lithosphere and the nearby Hainan plume, with respective supra- and sub-normal $\delta^{26}\text{Mg}$ values. From the perspective of Mg isotope, the mantles of the southwestern and eastern sub-basins are compositionally inhomogeneous, with their mantle evolutionary histories being distinct.

© 2020 Science China Press. Published by Elsevier B.V. and Science China Press. All rights reserved.

1. Introduction

The South China Sea (SCS), which covers an area of ~ 3.5 million km^2 , is the largest marginal basin in the western Pacific and lies at the junction of the Eurasian, Indian, Australian, and Pacific plates. Its opening and evolution during the Cenozoic involved geodynamic interactions between these major tectonic plates, the natures of which are still debated (Sun [1] and references therein). The nature of the mantle domain beneath the SCS is poorly constrained due to a lack of samples of seafloor igneous crust. The International Ocean Discovery Program (IODP) Expedition 349 drilled into the basement of the SCS oceanic crust, and recovered mid-ocean ridge basalts (MORBs) from the southwestern (Site

U1433) and eastern (Site U1431) sub-basins for the first time [2] (Fig. 1), aiding studies on the nature of the SCS sub-ridge mantle [3–10].

The lithologies of basalts from sites Site U1431 and Site U1433 involve predominantly normal (N) and enriched (E)-MORB, respectively. These MORBs have distinct geochemistries [3,4]. In this study, basalt Mg isotopic compositions provide novel perspectives of mantle compositional evolution in the SCS. Comprehensive and robust datasets concerning the compositions of diverse terrestrial reservoirs are available [11], enabling the use of Mg isotopic compositions of volcanic rocks in tracing surficial materials recycled to the deep mantle. Ocean-island basalt (OIB)-type rocks usually exhibit considerable compositional variability, with $\delta^{26}\text{Mg}$ values of -0.6‰ to -0.3‰ [12–16]. The Mg isotopic compositions of MORBs are relatively homogeneous, with a mean $\delta^{26}\text{Mg}$ value of $-0.25\text{‰} \pm 0.06\text{‰}$ (2SD; $n = 47$; Teng et al. [15]), which is identical

* Corresponding author.

E-mail address: zhangguoliang@qdio.ac.cn (G.-L. Zhang).

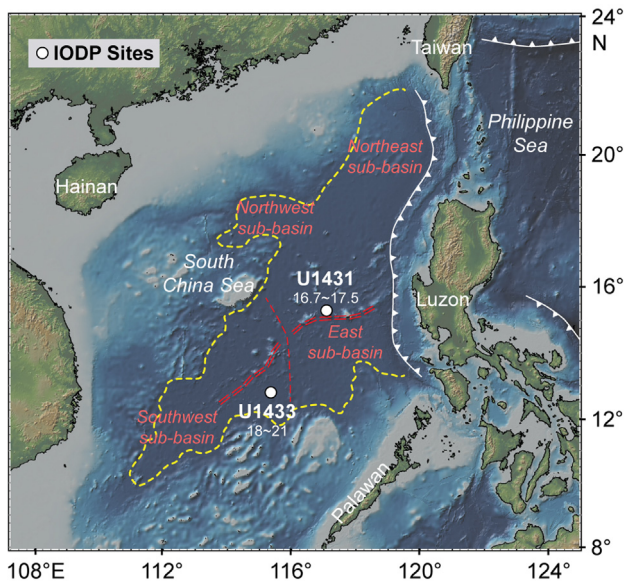


Fig. 1. Bathymetric map showing the South China Sea (SCS) and surrounding area. White curves and triangles denote subduction zones and direction, respectively. Yellow dotted line outlines the deep-water basin of the SCS. Red double-dashed line indicates the fossil spreading ridge, and single-dashed line the Zhongnan Fault, which divides the SCS basin into eastern and southwestern sub-basins. Numbers below site names indicate ages of drilled oceanic crust (Ma) [2]. Base map and bathymetric data are from <http://www.geomapp.org/>.

to that of normal mantle ($\delta^{26}\text{Mg} = -0.25\text{‰} \pm 0.04\text{‰}$; Teng [11]), although such a constraint on MORB $\delta^{26}\text{Mg}$ values may be due to a small dataset. Here we undertook, for the first time, Mg isotope analyses of fresh basalt samples from sites Site U1431 and Site U1433, with the aim of elucidating the origin of the large-scale mantle compositional heterogeneity of the SCS.

2. Geologic setting and samples

The SCS began opening at ca. 33 Ma and the subsequent seafloor spreading ceased at ca. 16 Ma [2]. The SCS includes four sub-basins: the northeastern, northwestern, eastern, and southwestern sub-basins (Fig. 1). The eastern and southwestern sub-basins are separated by the Zhongnan Fault and constitute the main SCS deep-water basin. Seafloor magnetic records indicate that the oceanic crust of the largest (eastern) sub-basin was accreted in N–S spreading during 33–16 Ma, and the V-shaped southwestern sub-basin was formed later by NW–SE spreading at 23.6–16.0 Ma [2].

The IODP Expedition 349 recovered igneous basement from Site U1431 (“Hole E”) in the eastern sub-basin and Site U1433 (“Hole B”) in the southwestern sub-basin, with the former being adjacent to the fossil ridge of the eastern sub-basin. Two independent basalt layers at 890.0–962.5 and 972.0–1007.9 m below seafloor (mbsf) were identified at Site U1431. The upper layer comprises sheet lavas containing abundant olivine cumulates, and the lower layer contains both sheet and pillow lavas with more limited crystallization of olivine [3]. At Site U1433, basalts appear at 786.3–858.5 mbsf as pillow lavas and massive lava flows with variable plagioclase phenocryst contents and minor olivine microphenocrysts [8] (Fig. S1 online).

Chondrite-normalized $(\text{La}/\text{Sm})_{\text{N}}$ ratios (based on normalization values of Anders and Grevesse [17]) indicate that seafloor basalts at Site U1431 include a large percentage of N-MORBs [$(\text{La}/\text{Sm})_{\text{N}} = 0.52\text{--}0.71$] and relatively rare E-MORBs [$(\text{La}/\text{Sm})_{\text{N}} = 1.29$], whereas those at Site U1433 are all E-MORBs [$(\text{La}/\text{Sm})_{\text{N}} = 1.00\text{--}1$].

02]. Compared with MORBs at Site U1431, those at Site U1433 are slightly more depleted in Sr–Nd–Hf isotopes and enriched in unradiogenic Pb isotopes, with respective means as follows: $^{87}\text{Sr}/^{86}\text{Sr} = 0.7031$ and 0.7030 ; $\epsilon_{\text{Nd}} = 7.84$ and 8.93 ; $\epsilon_{\text{Hf}} = 11.82$ and 15.16 ; and $^{206}\text{Pb}/^{204}\text{Pb} = 18.47$ and 17.69 [3,4]. In this study, ten seafloor basalt samples from Site U1431 and eight from Site U1433 were analyzed for Mg isotopes.

3. Methods

The Mg isotope analyses were respectively undertaken at the CAS Key Laboratory of Crust–Mantle Materials and Environments at the University of Science and Technology of China (USTC), and the Institute of Geology and Geophysics, Chinese Academy of Sciences (IGGCAS), following procedures described by An et al. [18] and summarized here. Rock sample and standard powders were weighed into Savillex screw-top beakers and dissolved in HF–HNO₃. The digestion residue was repeatedly evaporated with HCl–HNO₃ and HNO₃ and finally dissolved in 2 mol/L HNO₃ for column chemistry. Mg purification was achieved by cation exchange using 2 mL Bio-Rad AG50W-X12 resin (200–400 mesh), with the column procedure being repeated. Mg recoveries for samples and standards were $\geq 99.7\%$ and the total procedural Mg blank < 10 ng. Mg isotopic compositions were determined by multi-collector–inductively coupled plasma–mass spectrometry (MC–ICP–MS; Thermo-Finnigan Neptune; USA) using the sample–standard bracketing technique under wet plasma conditions. Samples were analyzed at least in triplicate, and results are expressed in the δ notation relative to the DSM3 standard (an Mg standard solution made from pure Mg metal [19]):

$$\delta^X\text{Mg} = \left(\left(\text{XMg}/^{24}\text{Mg} \right)_{\text{sample}} / \left(\text{XMg}/^{24}\text{Mg} \right)_{\text{DSM3}} - 1 \right) \times 1000\text{‰}, \quad (1)$$

where $X = 25$ or 26 . Long-term reproducibility and accuracy (at both laboratories) were better than 0.06‰ (2SD) for $\delta^{26}\text{Mg}$.

4. Results

The Mg isotopic compositions of SCS seafloor basalts and standards determined in this study are listed in Tables S1 and S2 (online), respectively (see also Fig. S2 online), with the latter being consistent with reference values reported by An et al. [18]. Table S1 (online) also includes critical previously published data [3,4], which are covered more widely in Table S3 (online).

The $\delta^{26}\text{Mg}$ values of the Site U1431 basalts range from -0.32‰ to -0.23‰ (average $-0.27\text{‰} \pm 0.06\text{‰}$; 2SD; $n = 10$), overlapping the normal mantle value of $-0.25\text{‰} \pm 0.04\text{‰}$ [11]. The Site U1433 basalt $\delta^{26}\text{Mg}$ values range from -0.24‰ to -0.15‰ (average $-0.20\text{‰} \pm 0.06\text{‰}$; 2SD; $n = 8$). A two-tailed t -test confirmed that the two sets of values are significantly different ($P < 0.01$ at 95% confidence level). Furthermore, the high- $\delta^{26}\text{Mg}$ endmember of the Site U1433 basalts ($\delta^{26}\text{Mg} = -0.15\text{‰} \pm 0.02\text{‰}$; 2SD) is beyond the normal mantle range (Fig. 2).

5. Discussion

5.1. Unusual $\delta^{26}\text{Mg}$ values of Site U1433 basalts

The $\delta^{26}\text{Mg}$ values of the Site U1433 basalts are systematically higher than those reported previously for fresh MORBs globally ($-0.25\text{‰} \pm 0.06\text{‰}$; 2SD; $n = 47$; [15]). Non-mantle-like $\delta^{26}\text{Mg}$ values of oceanic crust basalts are commonly attributed to seawater alteration and/or sediment contamination [20–23]. The unusual $\delta^{26}\text{Mg}$ values of the Site U1433 basalts are coupled with anomalous

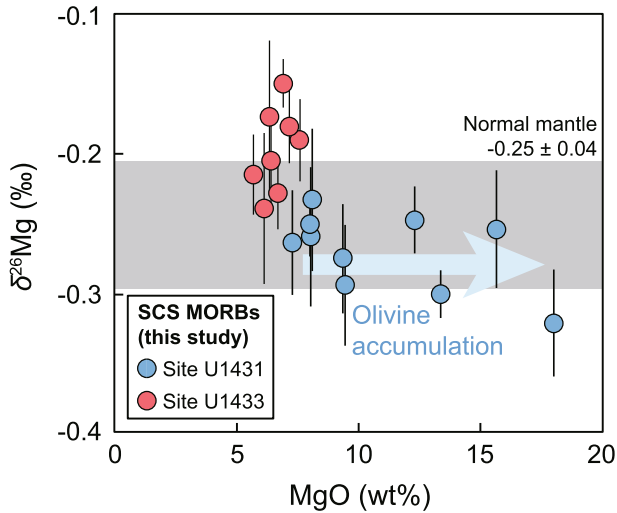


Fig. 2. $\delta^{26}\text{Mg}$ –MgO diagram for SCS MORBs highlighting the difference between the Site U1431 and Site U1433 basalts. The terrestrial mantle range (gray shaded) is from Teng [11]. The horizontal olivine accumulation trend of Site U1431 MORBs indicates olivine crystallization will not lead to Mg isotopic fractionation in the residual melt. Error bars represent 2SD uncertainties.

Pb isotopic compositions (Fig. 3). The following discussion considers whether the Mg isotopic compositions of the Site U1433 MORBs mirror upper-mantle sources or are masked by post-eruption weathering.

Altered oceanic crust samples (uncontaminated by sediment) have an average $\delta^{26}\text{Mg}$ value of $-0.18\text{‰} \pm 0.13\text{‰}$ (2SD; $n = 73$), with greater variability and a slightly higher average value than fresh samples [20–22]. Chemical weathering residues usually have high $\delta^{26}\text{Mg}$ values because secondary clay minerals preferentially scavenge heavy Mg isotopes from surrounding fluids [37], elevating $\delta^{26}\text{Mg}$ values of the altered basalts [38]. However, sample photomicrographs (Fig. S1 online) indicate that alteration of the Site U1433 basalt samples is negligible. This is further indicated by all of these basalts having (1) fairly low loss on ignition values (LOI < 1.5 wt%) and uniform chemical index of alteration values (CIA; molar $\text{Al}_2\text{O}_3/(\text{Al}_2\text{O}_3 + \text{CaO}_{\text{silicate}} + \text{Na}_2\text{O} + \text{K}_2\text{O})$ of 38.1–39.2; and (2) correlated alteration-sensitive/insensitive pairs of trace elements such as Th–U and Nb–Ba, which tend to be strongly decoupled in altered MORBs [39] (Fig. S3 online).

Magma differentiation may also cause a slight $\delta^{26}\text{Mg}$ shift (e.g., Schiller et al. [40]). However, high-MgO Site U1431 MORBs (MgO > 10.0 wt%) with strong olivine cumulation have a mean $\delta^{26}\text{Mg}$ value of -0.28‰ , whereas the low-MgO Site U1431 MORBs (MgO < 10.0 wt%) have more uniform $\delta^{26}\text{Mg}$ values (mean $-0.26\text{‰} \pm 0.04\text{‰}$; 2SD; $n = 6$). The identical Mg isotopic compositions of these two groups indicate that olivine cumulation and/or fractionation cannot cause a resolvable $\delta^{26}\text{Mg}$ deviation from the host magma. This is consistent with the fractionation behaviors of Mg isotopes observed in Hawaiian Kilauea Iki lavas [41].

Partial melting tends to fractionate Mg isotopes between melt and residual mantle sources in different molten mineral assemblages [22,42]. MORBs are high-degree partial melts typically formed in the spinel stability field of peridotitic mantle. Spinel is one of the major peridotite phases enriched in heavy Mg isotopes [30,31,43], so the fractionation effect on MORB magma of the melting of spinel peridotite requires consideration. We adopted the modelling method of Zhong et al. [22] and Williams and Bizimis [44] to investigate whether the melting of spinel-face peridotite could explain the elevated $\delta^{26}\text{Mg}$ values of the Site U1433 MORBs (modelling parameters are summarized in Table S4 online). Results indicate that the $\delta^{26}\text{Mg}$ values of melts are positively correlated

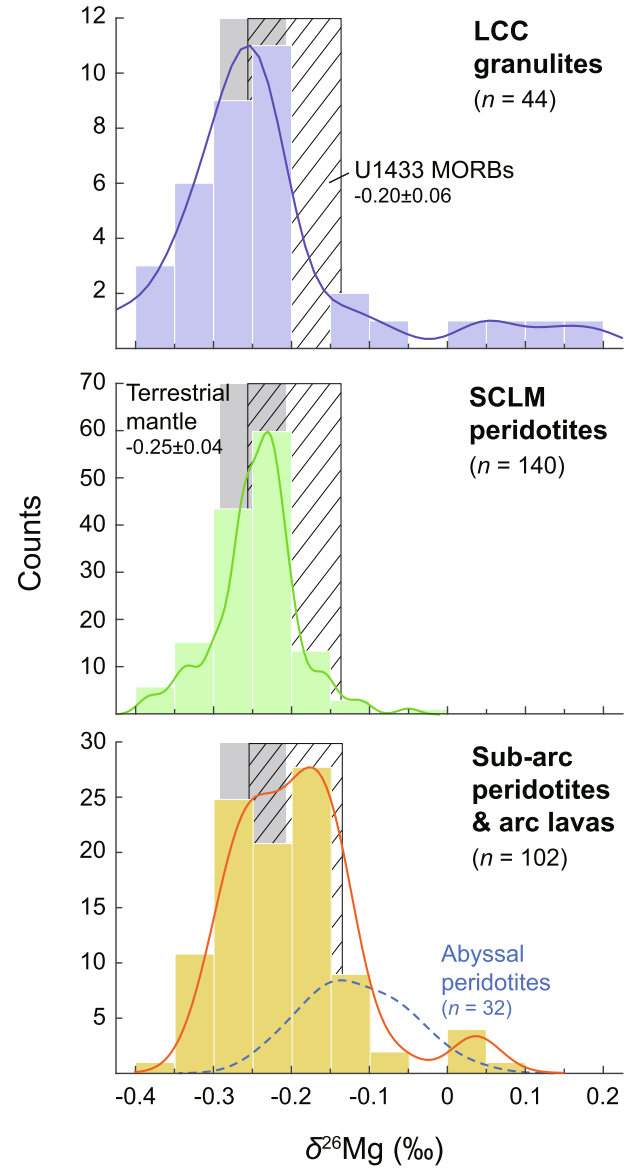


Fig. 3. Frequency distributions for Mg isotopic compositions of diverse terrestrial reservoirs. The range of $\delta^{26}\text{Mg}$ values was adjusted and some data excluded to optimize visual effectiveness. The colored curves are probability density functions calculated by MATLAB (R2018b). Grey-shaded and lined areas show the ranges of normal mantle [11] and Site U1433 MORBs. Data sources are: lower continental crust (LCC) granulites [24,25]; subcontinental lithospheric mantle (SCLM) peridotites [15,26–32]; sub-arc peridotites [28,33,34]; arc lavas [12,35] and abyssal peridotites [36].

with the degree of melting, with low-degree melts being slightly enriched in light Mg isotopes (Fig. S4 online). This is due to spinel being only a subsidiary mineral phase in peridotite, with clinopyroxene therefore contributing overwhelmingly to the melt [45]. The model results apparently conflict with the positive SCS MORB trend in the $\delta^{26}\text{Mg}$ –(La/Sm) diagram (Fig. S4 online), which indicates the Site U1433 E-MORBs, rather than the Site U1431 N-MORBs, are enriched in heavy Mg isotopes. We therefore consider that the difference between the Site U1431 and Site U1433 MORBs was not caused by partial melting of spinel peridotite. Having thus excluded the influence of seafloor weathering, mantle melting, and magmatic processes, we suggest that the unusually heavy Mg isotopic signature of the Site U1433 basalts was inherited from their mantle source.

5.2. The origin of the high- $\delta^{26}\text{Mg}$ Site U1433 basalts

The supra-mantle $\delta^{26}\text{Mg}$ values of the Site U1433 basalts were likely caused by the involvement of recycled components in their source, as they also have notable unradiogenic $^{206}\text{Pb}/^{204}\text{Pb}$ ratios (17.59–17.70) relative to MORBs of the East Pacific Rise (EPR; mean $^{206}\text{Pb}/^{204}\text{Pb} = 18.4$; [46]). The origin of such Indian-type Pb isotopic signatures (the “DUPAL anomaly” [47,48]) is still debated, with plausible suggestions including recycled pelagic sediments associated with oceanic crust [49], delaminated subcontinental lithospheric mantle (SCLM) [50,51], or lower continental crust (LCC) [52–54].

Ancient pelagic sediments are often considered possible source components for the mantle endmember “Enriched Mantle 1” (EM1), with very low $^{206}\text{Pb}/^{204}\text{Pb}$ ratios [55]. These sediments have $\delta^{26}\text{Mg}$ values that vary from heavy to light, depending on whether their predominant endmember is clay- or carbonate-rich [56,57]. A recent study of typical EM1-type Pitcairn shield lavas found that these ocean-island basalts (OIBs) with low $^{206}\text{Pb}/^{204}\text{Pb}$ ratios also have abnormally low $\delta^{26}\text{Mg}$ values of -0.40‰ to -0.31‰ , unlike the Site U1433 basalts [14]. Therefore, the unradiogenic Pb isotopic signature of the EM1 endmember is more likely associated with carbonate-bearing pelagic sediments, which would preserve light Mg isotopic signatures [57] even after being subducted into the deep mantle [58]. The differences in $\delta^{26}\text{Mg}$ values between the Site

U1433 MORBs and the Pitcairn lavas imply that carbonate-bearing pelagic sediments cannot account for the low $^{206}\text{Pb}/^{204}\text{Pb}$ ratios of the former.

Previous studies of Mg isotopic compositions of SCLM and LCC xenoliths have found that both may have subnormal $\delta^{26}\text{Mg}$ values associated with varying degrees of metasomatism (e.g., Pogge von Strandmann et al. [28]). However, only extensively metasomatized samples could have abnormal $\delta^{26}\text{Mg}$ values, and these are minor reservoir components. Most SCLM peridotites and LCC granulites have mantle-like $\delta^{26}\text{Mg}$ values, as the compiled dataset shows (Fig. 3). The Mg isotopic composition of melt generated by a high degree of melting should resemble the average value of the bulk source (also see Fig. S4 online), and the Site U1433 basalts would inherit mantle-like $\delta^{26}\text{Mg}$ values even if they were derived from mantle containing SCLM or LCC components. Therefore, we suggest that neither SCLM nor deep continental crust were responsible for the supra-normal $\delta^{26}\text{Mg}$ signatures of the Site U1433 basalts.

For a given MgO content, the Site U1433 basalts have higher CaO contents and CaO/Al₂O₃ ratios, and lower Fe₂O₃ contents, than the Site U1431 basalts (Fig. S5 online). Such differences in major-element composition suggest that the mantle source of the Site U1431 MORBs is peculiarly pyroxenitic (as also indicated by its olivine composition [3]), whereas the Site U1431 MORB source is normally peridotitic. This source lithological heterogeneity is also reflected in bulk-rock Fe/Mn ratios [59,60]. The negative

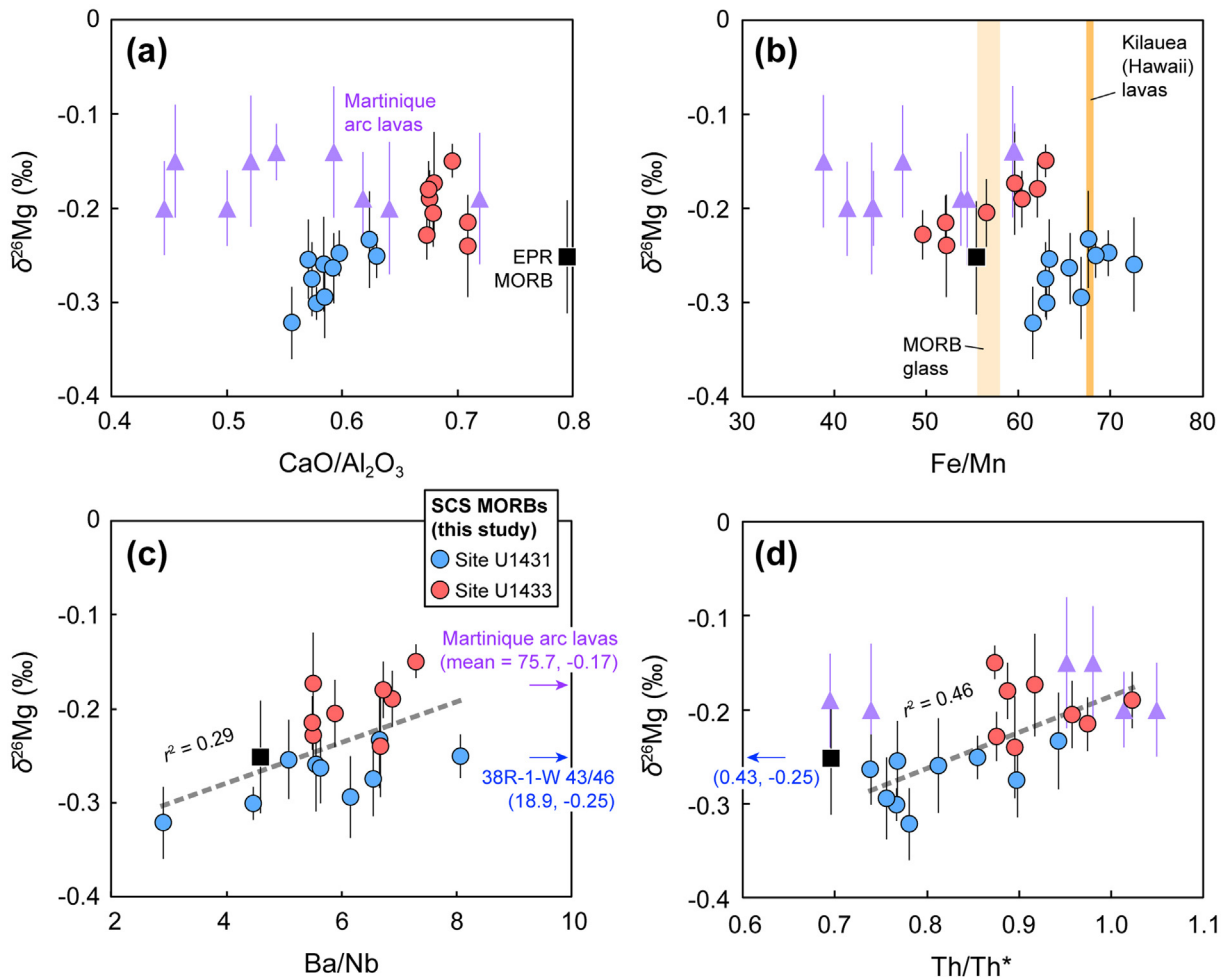


Fig. 4. $\delta^{26}\text{Mg}$ value versus whole-rock (a) CaO/Al₂O₃, (b) Fe/Mn, (c) Ba/Nb and (d) Th/Th* ratios for SCS MORBs. Th/Th* = $2 \times \text{Th}_N / (\text{Ba}_N + \text{La}_N)$, where the subscript N denotes the normalized value with respect to the primitive mantle [62]. The average Mg isotopic composition of EPR MORBs is from Teng et al. [15]; other data are from Gale et al. [46]. To reduce uncertainties in major-element and isotopic compositions caused by magma differentiation and source contamination, only low-silica Martinique arc samples (SiO₂ < 55 wt%) are plotted [35]. Shaded columns in (b) indicate the range of Fe/Mn ratios in oceanic basalts of different source lithology [63].

CaO–MgO correlation (Fig. S5 online) suggests that the fractionated mineral phase of the analyzed Site U1431 and Site U1433 MORBs is dominated by olivine. Their bulk-rock Fe/Mn ratios are thus controlled primarily by source lithology, rather than magmatic differentiation [61]. The $\delta^{26}\text{Mg}$ –(CaO/Al₂O₃) and $\delta^{26}\text{Mg}$ –(Fe/Mn) diagrams (Fig. 4a, b) indicate that the Site U1433 MORBs have high CaO/Al₂O₃ and low Fe/Mn ratios, similar to those of EPR MORBs [46]. The relatively heavy Mg isotopic composition is thus a common and inherent feature of the mantle peridotite tapped by the Site U1433 basalts.

The Mg isotopic compositions of lavas from the Martinique arc are generally heavier than that of normal mantle (mean $\delta^{26}\text{Mg}$ = $-0.18\text{‰} \pm 0.07\text{‰}$; 2SD; $n = 26$; [35]), implying that the sub-arc mantle is a plausible high- $\delta^{26}\text{Mg}$ peridotitic source for the Site U1433 basalts. Globally, island-arc basalts also have variable $\delta^{26}\text{Mg}$ values with a slightly supra-normal average of $-0.19\text{‰} \pm 0.25\text{‰}$ (2SD; $n = 29$) [12,35]. On the other hand, sub-arc peridotites display limited $\delta^{26}\text{Mg}$ variation from normal mantle to higher end-member values [28,33,34] (Fig. 3). Inter-arc Mg isotopic heterogeneity has been attributed to high-MgO fluids derived from high- $\delta^{26}\text{Mg}$ altered abyssal peridotites (Liu et al. [36]) (Fig. 3), rather than sediment-derived fluids, causing elevation of $\delta^{26}\text{Mg}$ values of the sub-arc mantle, as the latter are normally low in Mg content [64]. We infer that subduction zones exclusively produce large-scale heavy Mg isotopic anomalies in the upper mantle, given that (1) fluids released from the subducting slab commonly have $\delta^{26}\text{Mg}$ values above the normal mantle value, even though they are derived from subducting sediments [35,65], altered oceanic crust [66], or altered peridotites [67,68]; and (2) the interaction between slab-derived fluids and overlying mantle wedge must be secular and coherent to sufficiently elevate $\delta^{26}\text{Mg}$ values of high-MgO sub-arc peridotites.

Trace-element systematics of SCS MORBs exhibit higher Ba/Nb and lower Nb/Th ratios than those of EPR MORBs [46] and average depleted MORB mantle (DMM) [69] (Fig. S6 online). Such Ba and Th enrichment of their mantle source is consistent with the consequences of subduction modification [70], as clearly exemplified by seafloor basalts from the Lau back-arc basin [46] (Fig. S6 online). The $\delta^{26}\text{Mg}$ –(Ba/Nb) and $\delta^{26}\text{Mg}$ –(Th/Th*) diagrams (Fig. 4c, d) further indicate that, barring only one Site U1431 sample (Site U1431E-38R-1-W 43/46), SCS MORBs exhibit positive correlation between $\delta^{26}\text{Mg}$ and Ba/Nb ($r^2 = 0.29$) and Th/Th* ($r^2 = 0.46$). The supra-normal $\delta^{26}\text{Mg}$ values and peridotite-derived bulk-rock CaO/Al₂O₃ and Fe/Mn ratios, and subduction-modified Ba and Th excesses in the Site U1433 MORBs have also been found in low-SiO₂ (SiO₂ < 55.0 wt%) Martinique arc lavas [35] (Fig. 4). We therefore infer that the elevated $\delta^{26}\text{Mg}$ values of Site U1433 basalts originated from the sub-arc peridotitic mantle beneath the SCS southwestern sub-basin.

Recycled arc mantle relicts have recently been recovered from the Mid-Atlantic Ridge [71]. Although such components may constitute a major part of the upper mantle by volume, these highly refractory mantle domains are considered to contribute little to mantle melting [71], consistent with the observation that there is no resolvable difference in $\delta^{26}\text{Mg}$ values between MORBs of the Pacific, Atlantic, and Indian oceans (Fig. 5). Compared with mature ocean basins with seafloor-spreading histories of >100 Ma, the SCS southwestern sub-basin is a juvenile oceanic basin (24–16 Ma; [2]). The relatively high $\delta^{26}\text{Mg}$ values recorded in oceanic crust of this sub-basin thus indicate that the recycled sub-arc lithosphere is not refractory and could generate high- $\delta^{26}\text{Mg}$ melt during mantle melting in the initial spreading stage (Fig. 5), and all Site U1433 basalts being E-MORBs is consistent with preferential melting of enriched and fusible components. The Mg isotopic compositions of MORBs that formed during the initial extension stage could thus

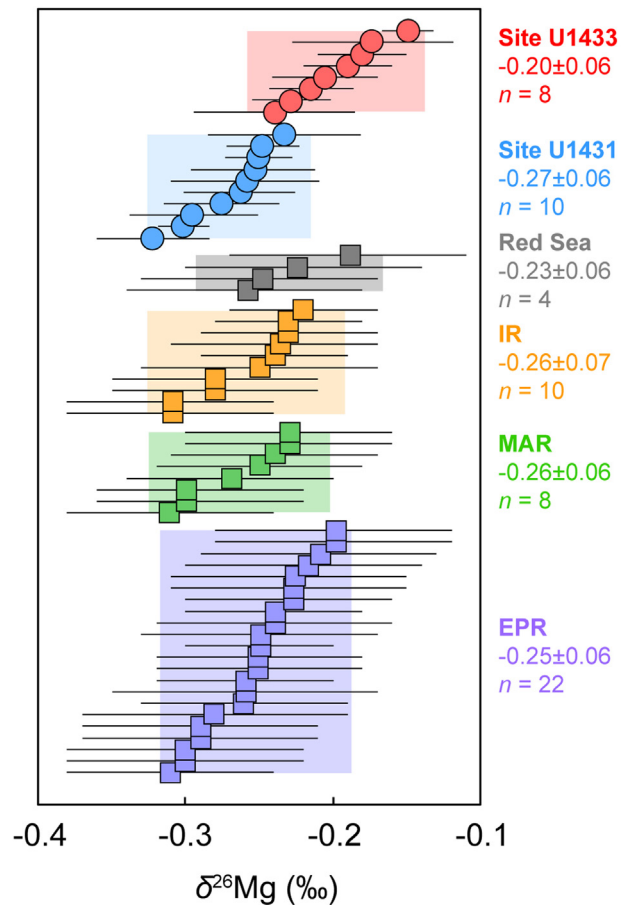


Fig. 5. Comparison between $\delta^{26}\text{Mg}$ values of MORB samples from global oceanic ridges [15] and the SCS (this study). Shaded backgrounds indicate the corresponding mean $\delta^{26}\text{Mg} \pm 2\text{SD}$ for each group, as also shown on the right. EPR = East Pacific Ridge, MAR = Mid-Atlantic Ridge, IR = Indian Ocean Ridge.

preserve precise information concerning recycled lithospheric components.

5.3. Distinct Mg isotopic signatures of the two sub-basins

Our statistical testing (Section 4) confirms a systematic difference in Mg isotopic composition between the Site U1431 and Site U1433 MORBs of the SCS eastern and southwestern sub-basins, respectively. The lower mean $\delta^{26}\text{Mg}$ value of the Site U1431 MORBs is also coupled with geochemical (i.e., Sr–Nd–Hf–Pb isotopes; Fig. 6) and lithological heterogeneity between mantle domains of the two sub-basins. The Site U1431 MORBs generally have slightly more enriched Sr–Nd–Hf isotopic compositions and more radiogenic Pb isotopic compositions (mean $^{87}\text{Sr}/^{86}\text{Sr} = 0.7031$; $\varepsilon_{\text{Nd}} = 7.84$; $\varepsilon_{\text{Hf}} = 11.82$; $^{206}\text{Pb}/^{204}\text{Pb} = 18.47$) than the Site U1433 MORBs (0.7030; 8.93; 15.16; 17.69, respectively) [4]. Based on the measured olivine compositions of the Site U1431 basalts, Zhang et al. [3] suggested that they were derived from an exotic pyroxenite-rich mantle source. This is also revealed by the relatively low bulk-rock Fe/Mn of Site U1431 MORBs (Fig. 4b). These multiple lines of evidence indicate that the lighter Mg isotopic compositions of the Site U1431 MORBs may be inherited from a recycled low- $\delta^{26}\text{Mg}$ source component, in which Sr–Nd–Hf isotopic compositions are more enriched and Pb more radiogenic than in the southwestern sub-basin mantle.

The compositional difference between MORBs of the two SCS sub-basins may be due to the influence on the SCS sub-ridge

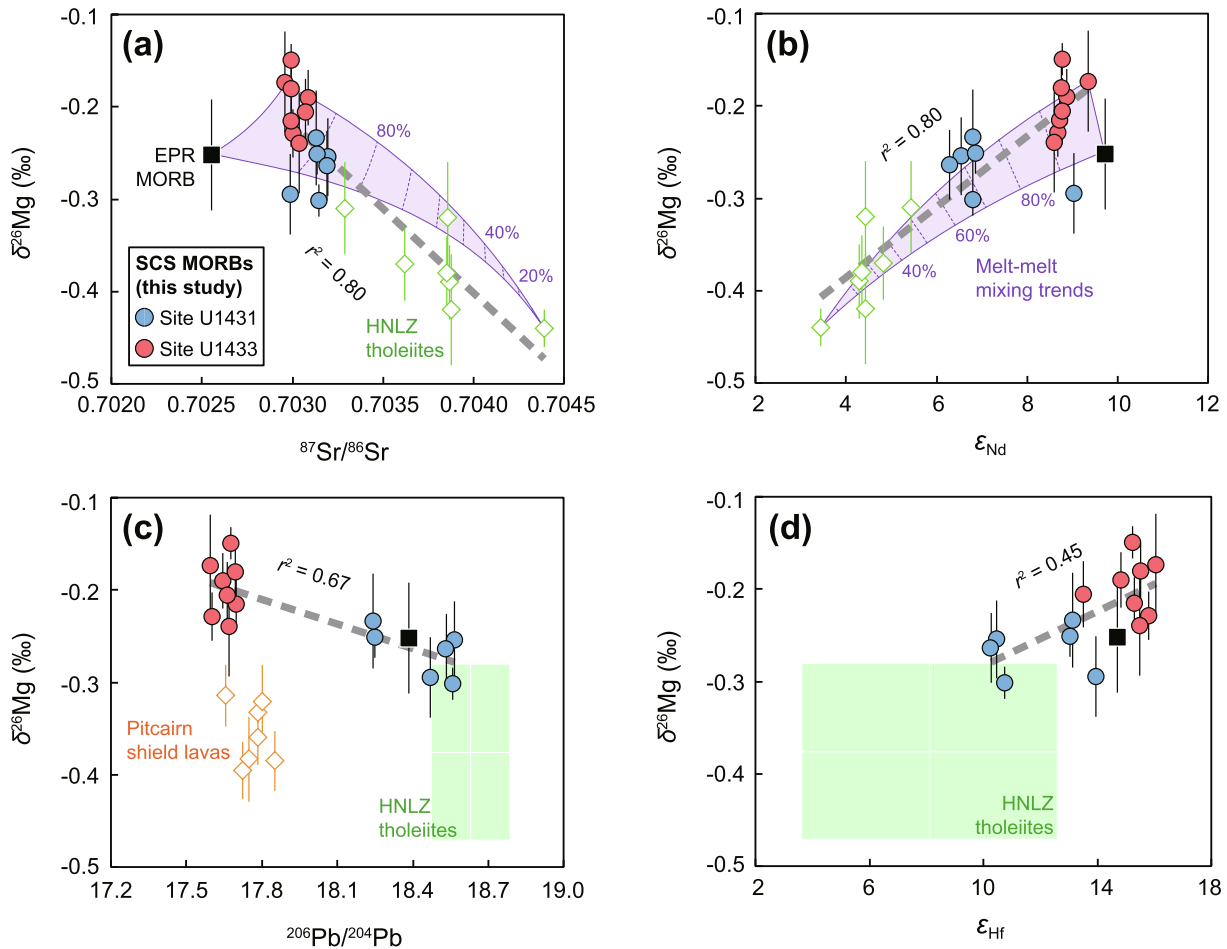


Fig. 6. $\delta^{26}\text{Mg}$ value versus radiogenic Sr–Nd–Pb–Hf isotopic compositions (indicated by $^{87}\text{Sr}/^{86}\text{Sr}$, ϵ_{Nd} , $^{206}\text{Pb}/^{204}\text{Pb}$, and ϵ_{Hf} values) for SCS MORBs. EPR MORB data are from Teng et al. [15]. Mg and Sr–Nd data for Hainan–Leizhou (HNLZ) tholeiites in (a) and (b) are from Li et al. [12]. The green-shaded areas in (c) and (d) illustrate the means \pm 2SD ranges on Mg–Pb–Hf isotopes of HNLZ tholeiites. The corresponding Pb and Hf isotopic data for the HNLZ samples with Mg isotopic compositions are absent and here we use the compiled data from Tu et al. [72], Zou and Fan [73], Wang et al. [74], and Sun et al. [75] instead. Mg and Pb isotopic compositions of Pitcairn shield lavas are from Wang et al. [14]. Purple curves and shaded areas in (a) and (b) depict the melt–melt mixing trends between the Site U1433 MORB (67R-1-W 55/58), HNLZ tholeiite (08HN-5C) and the average EPR MORB with 10% intervals (calculation parameters are given in Table S5 online).

mantle of a pyroxenite-rich mantle source feeding the intraplate Hainan hotspot (Fig. 1) [3]. The Hainan hotspot where volcanism commenced in the Hainan–Leizhou (HNLZ) area during the late Oligocene (28.4 Ma) [76], was much closer to Site U1431 than 16 Ma ago, so the HNLZ source component could have contributed to SCS MORB magmatism via plume–ridge interaction [3]. In that case, the enriched component of the eastern sub-basin mantle could have been constrained by voluminous post-spreading lavas in the HNLZ region. Previously published isotopic data indicate that post-spreading HNLZ basalts have Sr–Nd–Pb–Hf–Mg isotopic compositions of $^{87}\text{Sr}/^{86}\text{Sr} = 0.7030\text{--}0.7049$, $\epsilon_{\text{Nd}} = 2.3\text{--}8.0$, $^{206}\text{Pb}/^{204}\text{Pb} = 18.39\text{--}18.77$, $\epsilon_{\text{Hf}} = 5.5\text{--}12.0$, and $\delta^{26}\text{Mg} = -0.31\text{‰}$ to -0.58‰ [12,72–75]. These isotopic signatures also support the HNLZ component being a geochemically appropriate endmember accounting for compositional distinctions between the Site U1431 and Site U1433 MORBs. The Site U1431 and Site U1433 basalts and HNLZ tholeiites are strongly correlated in $\delta^{26}\text{Mg}$ – $^{87}\text{Sr}/^{86}\text{Sr}$, ϵ_{Nd} , $^{206}\text{Pb}/^{204}\text{Pb}$, and ϵ_{Hf} diagrams (Fig. 6). Each plot in Fig. 6 shows that the Site U1433 basalts and HNLZ tholeiites comprise the high- and low- $\delta^{26}\text{Mg}$ endmembers with coupled endmember-like Sr–Nd–Hf–Pb isotopic signatures. The Site U1431 basalts always occupy intermediate positions in these plots, indicating that their mantle-like $\delta^{26}\text{Mg}$ signatures result from mix-

ing of sub-arc peridotitic mantle (Site U1433 basalts) and pyroxenitic carbonated materials entrained in the Hainan hotspot (HNLZ tholeiites). A simple melt–melt mixing model applied between three endmembers (i.e., representative Site U1433 and Hainan samples and average EPR MORB) is also consistent with the covariation of Mg and Sr–Nd isotopic composition (Fig. 6a, b; mixing parameters are given in Table S5 online).

In summary, the Mg isotopically heavy sub-arc-type mantle inferred from the Site U1433 basalt compositions is the predominant endmember beneath the whole SCS basin, and the geochemical difference between sub-basins may be explained by extra injection of Hainan plume components into the mantle domain of the eastern sub-basin.

5.4. Pb–Mg isotopic anomaly associated with asthenosphere–lithosphere interaction

A mantle domain with low $^{206}\text{Pb}/^{204}\text{Pb}$ ratios and high $\delta^{26}\text{Mg}$ values (a common source endmember for SCS MORBs; Fig. 6) is consistent with the involvement of the buried root of a continental magmatic arc. Such an arc root has two components: a minor LCC-like component [4] that deposits abundant sulphides [77,78] to preserve unradiogenic Pb isotopes, and the sub-arc peridotitic

mantle with elevated $\delta^{26}\text{Mg}$ values. The low-MgO LCC-like component may have trace-element contents several orders of magnitude higher than those of high-MgO peridotites, producing a large-scale isotopically anomalous Pb domain retaining arc-type Mg isotopic signatures after sinking into the asthenospheric mantle.

Fragments of subduction-modified lithospheric mantle have been suggested as a possible low- $^{206}\text{Pb}/^{204}\text{Pb}$ source for MORBs of the Southwest Indian Ridge [51]. A similar model involving delaminated continental arc root has been proposed to explain the occurrence of low- $^{206}\text{Pb}/^{204}\text{Pb}$ volcanic glasses along the EPR [79]. Based on enrichment in mobile elements (Fig. S6 online), Richter et al. [80] identified an ancient subduction-modified mantle source for MORBs of Gakkel Ridge, Arctic Ocean, where $^{206}\text{Pb}/^{204}\text{Pb}$ ratios are also relatively low (~ 18.0). The heavy Mg isotopic compositions of fresh SCS MORBs provide convincing support for this hypothesis from an Mg isotopic perspective.

The compositional complexity of subduction-modified mantle wedge means that arc remnants may be an overlooked source of various types of geochemical imprint (other than unradiogenic Pb isotopes) for the sub-oceanic mantle, as partially validated by abnormal Li isotopic ratios of EPR basalts [81]. Globally, E-MORB sources generally carry sedimentary Ba isotopic compositions [82], and this Ba isotopic anomaly could also be preserved within the sub-arc mantle fluxed by enormous amounts of sediment-released fluids.

6. Concluding remarks

The Mg isotopic composition of the sub-ridge mantle of the SCS is heterogeneous on a sub-basin scale, consistent with the occurrence of radiogenic Sr–Nd–Pb isotopes. The Site U1431 MORBs of the eastern sub-basin have mantle-like Mg isotopic compositions, whereas the Site U1433 basalts of the southwestern sub-basin have variable and higher $\delta^{26}\text{Mg}$ values than the normal mantle. The distinctly heavy Mg isotopic signature of the Site U1433 basalts is consistent with that of arc remnants buried after Cenozoic continental rifting at the Euro–Asian continental margin. Such a high- $\delta^{26}\text{Mg}$ endmember is predominant in the upper SCS mantle, and the normal-mantle Mg isotopic compositions of the Site U1431 basalts may be explained by contamination by materials with sub-normal $\delta^{26}\text{Mg}$ values from the nearby Hainan plume. The Mg isotopic compositions thus indicate that the compositional inhomogeneity of the SCS upper mantle results from both shallow- and deep-level recycling, furthering the understanding of the distinct mantle evolutionary histories of the two SCS sub-basins.

Conflict of interest

The authors declare that they have no conflict of interest.

Acknowledgments

This work was financially supported by the Strategic Priority Research Program of the Chinese Academy of Sciences (XDA22050101, XDB42020302), the National Natural Science Foundation of China (91858206, 41876040), the Laboratory for Marine Geology, Qingdao National Laboratory for Marine Science and Technology (MGQNLN-TD201806) and the Taishan Scholars Program of Shandong Province (tsqn201909157). We thank the dedicated effort of the crew and scientific staff of the Drillship JOIDES Resolution. The laboratory and technical support afforded by Jin-Hui Yang, Yue-Heng Yang, Shi-Tou Wu at the Institute of Geology and Geophysics, Chinese Academy of Sciences, An-Xia Chen at the University of Science and Technology of China, and

Zhong-Biao Zhou, Xiao-Wen Liu at the Nanjing University is greatly appreciated. We are grateful to the helpful comments from two anonymous reviewers.

Author contributions

Yuan Zhong, Guo-Liang Zhang conceived the project. Yuan Zhong, Qi-Zhen Jin, Fang Huang, Xiao-Jun Wang and Lie-Wen Xie were responsible for the Mg isotopic measurements. All the authors contributed to the data interpretation and wrote the paper.

Appendix A. Supplementary materials

Supplementary materials to this article can be found online at <https://doi.org/10.1016/j.scib.2020.12.016>.

References

- [1] Sun W. Initiation and evolution of the South China Sea: an overview. *Acta Geochim* 2016;35:215–25.
- [2] Li C-F, Xu X, Lin J, et al. Ages and magnetic structures of the South China Sea constrained by deep tow magnetic surveys and IODP Expedition 349. *Geochem Geophys Geosyst* 2014;15:4958–83.
- [3] Zhang G-L, Sun W-D, Seward G. Mantle source and magmatic evolution of the dying spreading ridge in the South China Sea. *Geochem Geophys Geosyst* 2018;19:4385–99.
- [4] Zhang G-L, Luo Q, Zhao J, et al. Geochemical nature of sub-ridge mantle and opening dynamics of the South China Sea. *Earth Planet Sci Lett* 2018;489:145–55.
- [5] Wang W, Chu F, Wu X, et al. Constraining mantle heterogeneity beneath the South China Sea: a new perspective on magma water content. *Minerals* 2019;9:410.
- [6] Yu M, Yan Y, Huang CY, et al. Opening of the South China Sea and upwelling of the Hainan plume. *Geophys Res Lett* 2018;45:2600–9.
- [7] Zhang G-L, Chen L-H, Jackson MG, et al. Evolution of carbonated melt to alkali basalt in the South China Sea. *Nat Geosci* 2017;10:229–35.
- [8] Yang F, Huang X-L, Xu Y-G, et al. Magmatic processes associated with oceanic crustal accretion at slow-spreading ridges: evidence from plagioclase in mid-ocean ridge basalts from the South China Sea. *J Petrol* 2019;60:1135–62.
- [9] Yang F, Huang X-L, Xu Y-G, et al. Plume-ridge interaction in the South China Sea: thermometric evidence from Hole U1431E of IODP Expedition 349. *Lithos* 2019;324–325:466–78.
- [10] Sun K, Wu T, Liu X, et al. Lithochemistry of the mid-ocean ridge basalts near the fossil ridge of the southwest sub-basin, South China Sea. *Minerals* 2020;10:465.
- [11] Teng F-Z. Magnesium isotope geochemistry. *Rev Mineral Geochem* 2017;82:219–87.
- [12] Li S-G, Yang W, Ke S, et al. Deep carbon cycles constrained by a large-scale mantle Mg isotope anomaly in eastern China. *Natl Sci Rev* 2017;4:111–20.
- [13] Wang X-J, Chen L-H, Hofmann AW, et al. Mantle transition zone-derived EM1 component beneath NE China: geochemical evidence from Cenozoic potassic basalts. *Earth Planet Sci Lett* 2017;465:16–28.
- [14] Wang X-J, Chen L-H, Hofmann AW, et al. Recycled ancient ghost carbonate in the Pitcairn mantle plume. *Proc Natl Acad Sci USA* 2018;115:8682–7.
- [15] Teng F-Z, Li W-Y, Ke S, et al. Magnesium isotopic composition of the Earth and chondrites. *Geochem Cosmochim Acta* 2010;74:4150–66.
- [16] He Y, Chen LH, Shi JH, et al. Light Mg isotopic composition in the mantle beyond the big mantle wedge beneath eastern Asia. *J Geophys Res Solid Earth* 2019;124:8043–56.
- [17] Anders E, Grevesse N. Abundances of the elements: meteoritic and solar. *Geochem Cosmochim Acta* 1989;53:197–214.
- [18] An Y-J, Wu F, Xiang Y-X, et al. High-precision Mg isotope analyses of low-Mg rocks by MC-ICP-MS. *Chem Geol* 2014;390:9–21.
- [19] Galy A, Yoffe O, Janney PE, et al. Magnesium isotope heterogeneity of the isotopic standard SRM980 and new reference materials for magnesium-isotope-ratio measurements. *J Anal At Spectrom* 2003;18:1352–6.
- [20] Huang J, Ke S, Gao Y, et al. Magnesium isotopic compositions of altered oceanic basalts and gabbros from IODP Site 1256 at the East Pacific Rise. *Lithos* 2015;231:53–61.
- [21] Huang K-J, Teng F-Z, Plank T, et al. Magnesium isotopic composition of altered oceanic crust and the global Mg cycle. *Geochem Cosmochim Acta* 2018;238:357–73.
- [22] Zhong Y, Chen L-H, Wang X-J, et al. Magnesium isotopic variation of oceanic island basalts generated by partial melting and crustal recycling. *Earth Planet Sci Lett* 2017;463:127–35.
- [23] Ramos DPS, Coogan LA, Murphy JG, et al. Low-temperature oceanic crust alteration and the isotopic budgets of potassium and magnesium in seawater. *Earth Planet Sci Lett* 2020;541:116290.

- [24] Yang W, Teng F-Z, Li W-Y, et al. Magnesium isotopic composition of the deep continental crust. *Am Miner* 2016;101:243–52.
- [25] Teng F-Z, Yang W, Rudnick RL, et al. Heterogeneous magnesium isotopic composition of the lower continental crust: a xenolith perspective. *Geochem Geophys Geosyst* 2013;14:3844–56.
- [26] Yang W, Teng F-Z, Zhang H-F. Chondritic magnesium isotopic composition of the terrestrial mantle: a case study of peridotite xenoliths from the north China craton. *Earth Planet Sci Lett* 2009;288:475–82.
- [27] Bourdon B, Tipper ET, Fitoussi C, et al. Chondritic Mg isotope composition of the Earth. *Geochim Cosmochim Acta* 2010;74:5069–83.
- [28] Pogge von Strandmann PAE, Elliott T, Marschall HR, et al. Variations of Li and Mg isotope ratios in bulk chondrites and mantle xenoliths. *Geochim Cosmochim Acta* 2011;75:5247–68.
- [29] Huang F, Zhang Z, Lundstrom CC, et al. Iron and magnesium isotopic compositions of peridotite xenoliths from eastern China. *Geochim Cosmochim Acta* 2011;75:3318–34.
- [30] Xiao Y, Teng F-Z, Zhang H-F, et al. Large magnesium isotope fractionation in peridotite xenoliths from eastern North China Craton: product of melt–rock interaction. *Geochim Cosmochim Acta* 2013;77:115–241–61.
- [31] Liu S-A, Teng F-Z, Yang W, et al. High-temperature inter-mineral magnesium isotope fractionation in mantle xenoliths from the North China Craton. *Earth Planet Sci Lett* 2011;308:131–40.
- [32] An Y-J, Huang J-X, Griffin WL, et al. Isotopic composition of Mg and Fe in garnet peridotites from the Kaapvaal and Siberian cratons. *Geochim Cosmochim Acta* 2017;200:167–85.
- [33] Su B-X, Teng F-Z, Hu Y, et al. Iron and magnesium isotope fractionation in oceanic lithosphere and sub-arc mantle: perspectives from ophiolites. *Earth Planet Sci Lett* 2015;430:523–32.
- [34] Hu Y, Teng F-Z, Ionov DA. Magnesium isotopic composition of metasomatized upper sub-arc mantle and its implications to mg cycling in subduction zones. *Geochim Cosmochim Acta* 2020;278:219–34.
- [35] Teng F-Z, Hu Y, Chauvel C. Magnesium isotope geochemistry in arc volcanism. *Proc Natl Acad Sci USA* 2016;113:7082–7.
- [36] Liu P-P, Teng F-Z, Dick HJB, et al. Magnesium isotopic composition of the oceanic mantle and oceanic mg cycling. *Geochim Cosmochim Acta* 2017;206:151–65.
- [37] Ryu J-S, Vigier N, Decarreau A, et al. Experimental investigation of Mg isotope fractionation during mineral dissolution and clay formation. *Chem Geol* 2016;445:135–45.
- [38] Voigt M, Pearce CR, Fries DM, et al. Magnesium isotope fractionation during hydrothermal seawater–basalt interaction. *Geochim Cosmochim Acta* 2020;272:21–35.
- [39] Zhang G-L, Smith-Duque C. Seafloor basalt alteration and chemical change in the ultra thinly sedimented south Pacific. *Geochem Geophys Geosyst* 2014;15:3066–80.
- [40] Schiller M, Dallas JA, Creech J, et al. Tracking the formation of magma oceans in the solar system using stable magnesium isotopes. *Geochem Perspect Lett* 2017;3:22–31.
- [41] Teng F-Z, Wadhwa M, Helz RT. Investigation of magnesium isotope fractionation during basalt differentiation: implications for a chondritic composition of the terrestrial mantle. *Earth Planet Sci Lett* 2007;261:84–92.
- [42] Stracke A, Tipper ET, Klemme S, et al. Mg isotope systematics during magmatic processes: inter-mineral fractionation in mafic to ultramafic Hawaiian xenoliths. *Geochim Cosmochim Acta* 2018;226:192–205.
- [43] Young ED, Tonui E, Manning CE, et al. Spinel–olivine magnesium isotope thermometry in the mantle and implications for the Mg isotopic composition of Earth. *Earth Planet Sci Lett* 2009;288:524–33.
- [44] Williams HM, Bizimis M. Iron isotope tracing of mantle heterogeneity within the source regions of oceanic basalts. *Earth Planet Sci Lett* 2014;404:396–407.
- [45] Walter MJ, Sisson TW, Presnall DC. A mass proportion method for calculating melting reactions and application to melting of model upper mantle lherzolite. *Earth Planet Sci Lett* 1995;135:77–90.
- [46] Gale A, Dalton CA, Langmuir CH, et al. The mean composition of ocean ridge basalts. *Geochem Geophys Geosyst* 2013;14:489–518.
- [47] Hart SR. A large-scale isotope anomaly in the southern hemisphere mantle. *Nature* 1984;309:753–7.
- [48] Dupré B, Allègre CJ. Pb–Sr isotope variation in Indian Ocean basalts and mixing phenomena. *Nature* 1983;303:142–6.
- [49] Rehkämper M, Hofmann AW. Recycled ocean crust and sediment in Indian Ocean MORB. *Earth Planet Sci Lett* 1997;147:93–106.
- [50] Hawkesworth CJ, Mantovani MSM, Taylor PN, et al. Evidence from the Parana of south Brazil for a continental contribution to DUPAL basalts. *Nature* 1986;322:356–9.
- [51] Janney PE, Le Roex AP, Carlson RW. Hafnium isotope and trace element constraints on the nature of mantle heterogeneity beneath the central southwest Indian Ridge (13°E to 47°E). *J Petrol* 2005;46:2427–64.
- [52] Escrig S, Capmas F, Dupré B, et al. Osmium isotopic constraints on the nature of the DUPAL anomaly from Indian mid-ocean-ridge basalts. *Nature* 2004;431:59–63.
- [53] Hanan BB, Blichert-Toft J, Pyle DG, et al. Contrasting origins of the upper mantle revealed by hafnium and lead isotopes from the Southeast Indian Ridge. *Nature* 2004;432:91–4.
- [54] Gautheron C, Moreira M, Gerin C, et al. Constraints on the DUPAL anomaly from helium isotope systematics in the Southwest Indian mid-ocean ridge basalts. *Chem Geol* 2015;417:163–72.
- [55] Delavault H, Chauvel C, Thomassot E, et al. Sulfur and lead isotopic evidence of relic archean sediments in the Pitcairn mantle plume. *Proc Natl Acad Sci USA* 2016;113:12952–6.
- [56] Wang S-J, Teng F-Z, Rudnick RL, et al. The behavior of magnesium isotopes in low-grade metamorphosed mudrocks. *Geochim Cosmochim Acta* 2015;165:435–48.
- [57] Hu Y, Teng F-Z, Plank T, et al. Magnesium isotopic composition of subducting marine sediments. *Chem Geol* 2017;466:15–31.
- [58] Wang S-J, Teng F-Z, Li S-G. Tracing carbonate–silicate interaction during subduction using magnesium and oxygen isotopes. *Nat Commun* 2014;5:5328.
- [59] Sobolev AV, Hofmann AW, Kuzmin DV, et al. The amount of recycled crust in sources of mantle-derived melts. *Science* 2007;316:412–7.
- [60] Herzberg C, Asimow PD. Petrology of some oceanic island basalts: PRIMELT2. XLS software for primary magma calculation. *Geochem Geophys Geosyst* 2008;9:Q09001.
- [61] Le Roux V, Lee CTA, Turner SJ. Zn/Fe systematics in mafic and ultramafic systems: implications for detecting major element heterogeneities in the Earth's mantle. *Geochim Cosmochim Acta* 2010;74:2779–96.
- [62] McDonough WF, Sun SS. The composition of the Earth. *Chem Geol* 1995;120:223–53.
- [63] Humayun M, Qin L, Norman MD. Geochemical evidence for excess iron in the mantle beneath Hawaii. *Science* 2004;306:91.
- [64] Manning CE. The chemistry of subduction-zone fluids. *Earth Planet Sci Lett* 2004;223:1–16.
- [65] Wang S-J, Teng F-Z, Li S-G, et al. Tracing subduction zone fluid–rock interactions using trace element and Mg–Sr–Nd isotopes. *Lithos* 2017;290–291:94–103.
- [66] Huang J, Guo S, Jin Q-Z, et al. Iron and magnesium isotopic compositions of subduction-zone fluids and implications for arc volcanism. *Geochim Cosmochim Acta* 2020;278:376–91.
- [67] Chen Y-X, Schertl H-P, Zheng Y-F, et al. Mg–O isotopes trace the origin of Mg-rich fluids in the deeply subducted continental crust of Western Alps. *Earth Planet Sci Lett* 2016;456:157–67.
- [68] Chen Y-X, Demény A, Schertl H-P, et al. Tracing subduction zone fluids with distinct Mg isotope compositions: insights from high-pressure metasomatic rocks (leucophyllites) from the Eastern Alps. *Geochim Cosmochim Acta* 2020;271:154–78.
- [69] Workman RK, Hart SR. Major and trace element composition of the depleted MORB mantle (DMM). *Earth Planet Sci Lett* 2005;231:53–72.
- [70] Kessel R, Schmidt MW, Ulmer P, et al. Trace element signature of subduction-zone fluids, melts and supercritical liquids at 120–180 km depth. *Nature* 2005;437:724–7.
- [71] Urann BM, Dick HJB, Parnell-Turner R, et al. Recycled arc mantle recovered from the Mid-Atlantic Ridge. *Nat Commun* 2020;11:3887.
- [72] Tu K, Flower MFJ, Carlson RW, et al. Sr, Nd, and Pb isotopic compositions of Hainan basalts (south China): implications for a subcontinental lithosphere Dupal source. *Geology* 1991;19:567–9.
- [73] Zou H, Fan Q. U–th isotopes in Hainan basalts: implications for sub-asthenospheric origin of EM2 mantle endmember and the dynamics of melting beneath Hainan Island. *Lithos* 2010;116:145–52.
- [74] Wang X-C, Li Z-X, Li X-H, et al. Identification of an ancient mantle reservoir and young recycled materials in the source region of a young mantle plume: implications for potential linkages between plume and plate tectonics. *Earth Planet Sci Lett* 2013;377–378:248–59.
- [75] Sun P, Niu Y, Guo P, et al. Multiple mantle metasomatism beneath the Leizhou Peninsula, south China: evidence from elemental and Sr–Nd–Pb–Hf isotope geochemistry of the late Cenozoic volcanic rocks. *Int Geol Rev* 2019;61:1768–85.
- [76] Ho K-S, Chen J-C, Juang W-S. Geochronology and geochemistry of late Cenozoic basalts from the Leiqiong area, southern China. *J Asian Earth Sci* 2000;18:307–24.
- [77] Lee C-T-A, Luffi P, Chin EJ, et al. Copper systematics in arc magmas and implications for crust–mantle differentiation. *Science* 2012;336:64–8.
- [78] Richards JP. Postsubduction porphyry Cu–Au and epithermal Au deposits: products of remelting of subduction-modified lithosphere. *Geology* 2009;37:247–50.
- [79] Mougél B, Agranon A, Hemond C, et al. A highly unradiogenic lead isotopic signature revealed by volcanic rocks from the East Pacific Rise. *Nat Commun* 2014;5:4474.
- [80] Richter M, Nebel O, Maas R, et al. An early cretaceous subduction-modified mantle underneath the ultraslow spreading Gakkel Ridge, Arctic Ocean. *Sci Adv* 2020;6:eabb4340.
- [81] Elliott T, Thomas A, Jeffcoate A, et al. Lithium isotope evidence for subduction-enriched mantle in the source of mid-ocean-ridge basalts. *Nature* 2006;443:565–8.
- [82] Nielsen SG, Horner TJ, Pryor HV, et al. Barium isotope evidence for pervasive sediment recycling in the upper mantle. *Sci Adv* 2018;4:eas8675.



Yuan Zhong received his Ph.D. degree at School of Earth Sciences and Engineering, Nanjing University. He is currently a postdoctoral fellow of Center of Deep Sea Research, Institute of Oceanology, Chinese Academy of Sciences. His research interest includes stable metal isotope systematics and their applications in high-temperature mantle geochemical studies.



Guo-Liang Zhang received his Ph.D. degree at Institute of Oceanology, Chinese Academy of Sciences. He is currently a researcher of Center of Deep Sea Research, Institute of Oceanology, Chinese Academy of Sciences. His research interest includes sub-ridge magmatism and geodynamics of the asthenosphere, global intra-plate volcanism and mantle heterogeneity, genetic mechanism of subduction-related magmatism and deep carbon cycling processes in the magmatic activities.